End-Group Effects on the Structure and Spectroscopy of Oligoazines

William B. Euler,* Meng Cheng, and Chao Zhao

Department of Chemistry, 51 Lower College Road, University of Rhode Island, Kingston, Rhode Island 02881

Received September 15, 1999. Revised Manuscript Received October 21, 1999

Oligoazines with three different types of end groups, ketone, hydrazone, and 2-pyridine, are studied in solution. When the end groups are ketone or 2-pyridine, the ^{1}H and ^{13}C NMR spectra are simple and show that the oligomers maintain 2-fold symmetry up to the longest chain lengths investigated (five azine units for the 2-pyridine end groups). In contrast, when the end groups are hydrazones, the ^{1}H NMR spectra show evidence for as many as five conformers present in solution for each oligomer while the ^{13}C NMR spectra are still simple, indicative of a single compound. Semiempirical AM1 calculations suggest that all of the oligoazines should be severely twisted but give no insight about the origin of the large number of conformers found for the materials with hydrazone end groups. The end groups have a significant effect on the UV spectra. All the oligoazines show two absorptions close in energy, but the relative intensities change depending upon the end group. For ketone end groups the higher energy transition is stronger, for 2-pyridine end groups the lower energy transition dominates, and for the hydrazone end groups the two transitions are about the same intensity. Deconvolution of the UV spectra allowed a more accurate assessment of the profile of each absorption peak. Use of the fitting parameters for the lowest energy azine $\pi-\pi^*$ transition removed the effect of the end groups and gave a consistent estimate of the band gap in a poly(methylazine) of 3.31 eV.

Introduction

Polyazines, $-[C(R)=N-N=C(R)]_n-$, are air stable polymers with alternating imine bonds but with limited conjugation length.[1] The moderate delocalization along the chain is due, at least in part, to the low rotational barrier about the N−N bond.[2] Thus, although formally isoelectronic with polyacetylene, the polyazines do not undergo oxidative doping with iodine. Rather, these materials react with I_2 to form iodonium complexes.[3] Consequently, doped polyazines are poor electrical conductors.[4] However, polyazines do contain a diimine linkage that potentially could be used to chelate to transition metals. This could serve a dual purpose: to restrict rotations and to provide a method to influence the electronic structure of the polymer by varying the charge or bonding properties of the chelated metal complex.

We also found recently that the end group can have a profound effect on the structure of the azine linkage.[2] In the study of the crystal structures of 2-pyridinecarboxaldehydeazine and biacetylazine, it was found that when the end groups were 2-pyridines, the molecule crystallized into a planar state but when the end groups were ketones, the structure was twisted around the N−N bond. Semiempirical calculations showed that the energy of the molecule as it is rotated about the N−N bond was very broad about the minimum so that any number of small influences could change the structure of the azine.

In this work, we further explore the end-group effects on the structure and electronic spectroscopy of oligoazines. Three series of materials were synthesized, $R-[C(CH_3)=N-N=C(CH_3)]_n-R$ with R = $-C(CH_3)=O$ (**I-*n***), R = $-C(CH_3)=NNH_2$ (**II-*n***), and R = −(2-pyridine) (**III-*n***). The solution ^{1}H NMR spectra show single conformers for R = $-C(CH_3)=O$ and R = −(2-pyridine) for most values of *n* but a plethora of structures present for R = $-C(CH_3)=NNH_2$ for all chain lengths. Semiempirical AM1 calculations imply that all the oligoazines here have twisted conformations. The solution electronic spectra can be deconvoluted into only a few absorption bands, but the end groups cause shifts in each of these peaks, as well.

(1) (a) Euler, W. B.; *Sol. State Commun.* **1988**, *68*, 291−293. (b) Euler, W. B.; King, G. S. *Macromolecules* **1989**, *22*, 4664−4666. (c) Euler, W. B.; Gill, B. C. *Advanced Organic Solid State Materials*; Chiang, L. Y.; Chaikin, P. M.; Cowan, D. O.; Eds.; Materials Research Society Symposium Proceedings; **1990**, *173*, 375−378. (d) Euler, W. B.; Szabo, A. *Solid State Commun.* **1991**, *79*, 547−549. (e) Sherman, B. C.; Schmitz, B. K.; Euler, W. B. *Chem. Mater.* **1995**, *7*, 806−812. (f) Euler, W. B. *Handbook of Organic Conductive Molecules and Polymers*; Nalwa, H. S.; Ed.; John Wiley & Sons: Chichester, 1997; Vol. 2, pp 719−740.

(2) (a) Chen, G. S.; Anthamatten, M.; Barnes, C. L.; Glaser, R. *Angew. Chem., Int. Ed. Engl.* **1994**, *33*, 1081−1084. (b) Kesslen, E. C.; Euler, W. B.; *Tetrahedron Lett.* **1995**, *36*, 4725−4728. (c) Kesslen, E. C.; Euler, W. B.; Foxman, B. M. *Chem. Mater.* **1999**, *11*, 336−340.

(3) (a) Sherman, B. C.; Euler, W. B. *Chem. Mater.* **1994**, *6*, 899−906. (b) Euler, W. B. *Chem. Mater.* **1996**, *8*, 554−557.

(4) (a) Lee, Y. K.; Chung, H. S. *Polymer (Korea)* **1985**, *9*, 117−124. (b) Hauer, C. R.; King, G. S.; McCool, E. L.; Euler, W. B.; Ferrara, J. D.; Youngs, W. J. *J. Am. Chem. Soc.* **1987**, *109*, 5760−5765. (c) Cao, Y.; Li, S. *J. Chem. Soc., Chem. Commun.* **1988**, 937−938. (d) Euler, W. B. *Chem. Mater.* **1990**, *2*, 209−213. (e) Chaloner-Gill, B.; Cheer, C. J.; Roberts, J. E.; Euler, W. B. *Macromolecules* **1990**, *23*, 4597−4603.

10.1021/cm9905702 CCC: $18.00
Published on Web 12/02/1999

Table 1. Room Temperature ^{1}H NMR Spectra (400 MHz, $CDCl_3$) for R−[C(CH_3)=N−N=C(CH_3)]$_n$−R[a]

	δ(CH_3)	δ(CH_3)	δ(CH_3)	δ(CH_3)	δ(CH_3)	δ(NH_2)	δ(ring) (J, Hz)			
				I-*n* (R = −C(CH_3)=O)						
I-1	2.474				1.832					
I-2	2.486			2.042	1.861					
I-3	2.492		2.086	2.058	1.875					
I-4	2.496	2.104	2.092	2.065	1.878					
				II-*n* R = (−C(CH_3)=N−NH_2)						
II-1	2.094	2.064	2.055	1.993	1.950	5.598				
	2.090			1.984						
	2.082			1.977						
	2.075									
II-2	2.105	2.073	2.053	1.991	1.947	5.604				
	2.101	2.066		1.983						
	2.093	2.063		1.975						
	2.088									
	2.080									
II-3	2.109	2.074	2.054	1.997	1.951	5.613				
	2.107	2.071		1.992						
	2.103	2.064		1.984						
	2.094			1.976						
	2.089									
	2.081									
				III-*n* (R = 2-pyridine)						
III-1	2.373						8.652 (4.76)	8.237 (8.06)	7.766 (8.06, 7.30, 1.84)	7.325 (7.32, 4.76, 1.12)
III-2	2.344	2.180					8.653 (4.76)	8.207 (7.72)	7.770 (8.44, 7.32, 1.84)	7.331 (7.32, 4.76, 1.12)
III-3	2.327	2.154	2.149 2.144 (sh)	2.127			8.636 (4.80)	8.191 (8.04)	7.748 (8.04, 7.34, 1.84)	7.311 (7.32, 4.76)
III-4	2.322	2.148	2.140	2.121			8.631 (4.40)	8.186 (7.68)	7.742 (7.68, 7.52)	7.305 (8.04, 4.40)
III-5	2.353	2.157	2.141	2.125	2.122		8.671 (4.40)	8.214 (8.04)	7.802 (8.04, 7.68)	7.361 (7.68, 4.40)

[a] Chemical shifts are referenced to TMS. Coupling constants are given in parentheses in Hz.

Experimental Section

Materials were prepared by published methods.[2b,4b] ^{1}H and ^{13}C NMR spectra were run in $CDCl_3$ on a JEOL Eclipse 400 spectrometer operating at 400 MHz for ^{1}H and 100 MHz for ^{13}C and are referenced against TMS. Infrared spectra were run in $CHCl_3$ solution using a 1 mm path length cell with KBr windows on a Perkin-Elmer 1650 FTIR spectrometer between 400 and 4000 cm^{-1}. Electronic spectra were run in methanol on a Perkin-Elmer Lambda 900 spectrometer between 200 and 600 nm. UV spectra were fit to Gaussian line shapes using the fitting routines in SigmaPlot, version 4 (Jandel Scientific). AM1 and HF (using the 6-31G(*) basis set) calculations were performed using PCSpartan Plus software.[5] Frequency calculations showed that all structures found were at minima.

Results and Discussion

The oligoazines **I-*n*** and **III-*n*** were prepared by addition of an excess of 2,3-butanedione or 2-acetylpyridine to a dihydrazone (or hydrazine hydrate, for n = 1), starting with 2,3-butanedihydrazone.[2b,4b] Dihydrazones are prepared by reacting the diketones (**I-*n***) with excess hydrazine hydrate. In this fashion, any chain length oligomer can be synthesized up to the solubility

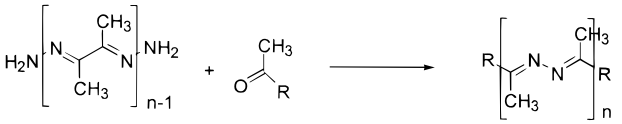

limits of the products. The following compounds were studied for this work: R = −C(CH_3)=O, n = 1−4 (**I-1** to **I-4**); R = −C(CH_3)=N−NH_2, n = 1−3 (**II-1** to **II-3**); and R = −C(CH_3)−(2-C_5H_4N), n = 1−5 (**III-1** to **III-5**). Although compound **II-4** was also prepared, it is not included in this study because of insufficient solubility.

The room-temperature ^{1}H NMR chemical shifts and coupling constants for all the compounds are listed in Table 1. If the oligoazines were planar, or at least have 2-fold symmetry, then the number of methyl resonances should be n for compounds **III-*n*** and n + 1 for compounds **I-*n*** and **II-*n***. This pattern is followed for **I-*n*** and **III-*n*** (except **III-3**) but compounds **II-*n*** have far more methyl resonances than expected for the structure. This was not due to impurities for three reasons: reaction of **II-*n*** to give **I-*n*+1** led to clean spectra without purification; the ^{13}C NMR spectra of compounds **II-*n*** showed single compounds; and raising the temperature broadened the spectra. Thus, compounds **II-*n*** at room temperature must be a mixture of several conformations in solution.

(5) PC Spartan Plus, 1.5 Wavefunction, Inc., 18401 Von Karman Ave., Ste. 370, Irvine, CA 92612. For background on the AM1 method, see: Dewar, M. J. S.; Zoebisch, E. G.; Healy, E. F.; Stewart, J. J. P. *J. Am. Chem. Soc.* **1985**, *107*, 3902−3909.

The chemical shift assignments for **I-*n*** are made as follows. The most deshielded peaks (2.474−2.496 ppm) arise from the methyl group bonded to the carbonyl carbon. On the basis of compound **I-1**, the most shielded resonances (1.832−1.878 ppm) must arise from the methyl groups attached to the azine carbons adjacent to the carbonyl end group. Then, as the chain length becomes longer, the methyl groups on azine groups more removed from the end group become increasingly deshielded. Even for **I-4** there is an easily observable difference between all of the methyl resonances.

The ^{1}H NMR spectra for compounds **II-*n*** are significantly more complex. The peak at 1.949 ± 0.002 ppm is assigned to the methyl groups on the hydrazone end group based on comparison to 2,3-butanedione dihydrazone (1.951 ppm). The remaining myriad of peaks break into two groups, above and below 2 ppm. No specific assignments can be made, but clearly a large number of conformers are present in solution. This was somewhat surprising since previous work on the ^{13}C solid-state NMR did not show evidence of multiple conformers.[6] This could be attributed to the larger line width found in solid-state spectra that hide the number of contributions to each observed resonance or the possibility that only single structures arise in the solid materials (compared to multiple conformations in solution).

The situation is mixed for **III-*n***. Except for a small but discernible shoulder in **III-3**, the methyl resonances in **III-*n*** are similar to **I-*n*** in the sense that 2-fold symmetry is apparent. However, the chemical shift variation as the chain length increases is not nearly as monotonic as in **I-*n***. Clearly, on the basis of **III-1**, the methyl group adjacent to the pyridine ring is the most deshielded and as the chain length increases, the interior methyl carbons become increasingly shielded, in direct contrast to **I-*n***. Nonetheless, it seems that both sets of compounds converge to about the same chemical shift for a methyl group on an infinitely long polyazine of about 2.12 ppm. The ring protons are similar for all compounds and can be assigned on the basis of the chemical shifts and the spin−spin splittings (given in parentheses in Table 1). The resonances at 8.6 and 8.2 ppm are doublets that must be associated with positions 3 and 6. The 8.6 ppm resonance is assigned to position 6, adjacent to the pyridine nitrogen, which then unambiguously assigns the other absorptions as position 3, 8.2 ppm, position 4, 7.75 ppm, and position 5, 7.3 ppm. There is no simple pattern in the chemical shifts or coupling constants as a function of chain length.

The temperature dependence of the ^{1}H NMR spectra helps confirm the hypothesis that the oligoazines easily attain multiple conformations in solution, although all three series of compounds behave differently. Between −25 °C and +50 °C compounds **I-*n*** give spectra that have small chemical shift changes in some peaks but the number of resonances is independent of temperature. We also observed evidence of decomposition in some samples. In contrast, the spectra of compounds **II-*n*** become broader with increased temperature and at +50 °C all three samples are near coalescence. This is consistent with the hypothesis of multiple conformations. Finally, compounds **III-*n*** showed no changes in the number of peaks at low temperatures but decomposed at +50 °C.

The room-temperature ^{13}C NMR resonances are given in Table 2. For all compounds, the resonances associated with the end groups were invariant as a function of increasing chain length. Further, for compounds **I-*n*** (n = 1−4), **II-*n*** (n = 1−3), and **III-*n*** (n = 1−3) the number of imine carbon and methyl carbon resonances exactly match the number expected for a single isomer (n for **I**−**n** and **III-*n***, n + 1 for **II-*n***). For compounds **III-4** and **III-5**, the number of imine (three and four peaks, respectively) and methyl (three peaks) resonances are less than expected, presumably because for these longest chain compounds the interior azines no longer experience the effect of the end group, as probed by the ^{13}C NMR, and the signals overlap. Most importantly, since single isomers are observed for **II-*n*** in the ^{13}C NMR spectra but multiple isomers are found in the ^{1}H NMR spectra, rotational averaging must be occurring for these compounds at room temperature.

The trends in the chemical shifts of the carbons associated with the azine groups give some insight into the bonding in these systems. In the methyl region, as the chain length increases, the chemical shifts cluster into two groups for each type of carbon and for each type of end group. For **I-*n***, with the carbonyl end groups, the methyl groups attached to the imine carbons show one shielded resonance (11.36−11.54 ppm) and a group (for compounds with more repeat units) of resonances clustered around 12.97 ± 0.14 ppm. The most reasonable assignment, then, for the 11.40 ± 0.14 ppm peak is to the methyl group adjacent to the end group, −N=C(*C*H$_3$)−C(CH$_3$)=O. The same type of pattern holds for **III-*n***, but with the unique resonance being the most deshielded at 13.89 ± 0.05 ppm and the cluster of resonances growing in at 12.95 ± 0.07 ppm. Again, the reasonable assignment is that the methyl group adjacent to the end group, −N=C(*C*H$_3$)−(2-pyr), is found at 13.89 ± 0.05 ppm. Such a simple pattern is not found for compounds **II-*n*** in the methyl region, although as the chain length increases the methyl peaks are becoming more shielded. In long-chain polyazines, in the solid state, the limiting methyl resonance is found at 12.6 ppm,[6b] in agreement with the solution values found here. This implies that interactions between chains in the solid state are small or, coincidentally, are remarkably similar to chloroform solvation.

The resonances in the imine region of the spectrum also show a convergence to the long-chain solid-state chemical shift. For compounds **I-*n***, as the chain length increases the resonances associated with the imine carbons become increasingly deshielded as the effect of the carbonyl end group becomes increasingly remote. In contrast, for both **II-*n*** and **III-*n***, the imine resonances become more shielded as the number of repeat units increase. All three sets of compounds appear to be converging to a value of about 156 ppm for an infinite chain, in agreement with the solid-state value measured to be 155.2 ppm.[6b]

(6) (a) Euler, W. B.; Roberts, J. E. *Synth. Met.* **1989**, *29*, E545−E549. (b) Euler, W. B.; Roberts, J. E. *Macromolecules* **1989**, *22*, 4221−4225. (c) Chaloner-Gill, B.; Euler, W. B.; Roberts, J. E. *Macromolecules* **1991**, *24*, 3074−3080. (d) Chaloner-Gill, B.; Euler, W. B.; Mumbauer, P. D.; Roberts, J. E. *J. Am. Chem. Soc.* **1991**, *113*, 6831−6834.

Table 2. Room-Temperature ^{13}C NMR Spectra (100 MHz, $CDCl_3$) for R−[C(CH$_3$)=N−N=C(CH$_3$)]$_n$−R[a]

I-*n* (R = −C(CH$_3$)=O)

	−*C*(CH$_3$)=O	−(*C*H$_3$)=O	−*C*(CH$_3$)=N−	−C(*C*H$_3$)=N−
I-1	197.38	24.76	152.37	11.54
I-2	197.98	24.86	153.47	11.42
			154.46	13.06
I-3	198.03	24.86	153.87	11.37
			154.40	12.87
			155.39	13.10
I-4	198.05	24.86	153.95	11.36
			154.42	12.83
			155.24	12.91
			155.78	13.11

II-*n* (R = −C(CH$_3$)=N−NH$_2$)

	−*C*(CH$_3$)=N−NH$_2$	−C(*C*H$_3$)=N−NH$_2$	−*C*(CH$_3$)=N−	−C(*C*H$_3$)=N−
II-1	147.62	8.63	156.98	12.39
II-2	147.15	8.61	156.55	12.57
			156.58	12.67
II-3	147.04	8.60	155.90	12.60
			156.33	12.65
			156.69	12.84

III-*n* (R = 2-pyridine)

	ring *C*2	ring *C*3	ring *C*4	ring *C*5	ring *C*6	−*C*(CH$_3$)=N−	−C(*C*H$_3$)=N−
III-1	155.74	121.25	136.29	124.11	148.74	157.57	13.94
III-2	155.57	121.25	136.29	124.14	148.75	156.64	13.02
						156.92	13.86
III-3	155.53	121.23	136.27	124.15	148.76	155.89	12.88
						156.68	12.96
						156.73	13.84
III-4	155.53	121.24	136.29	124.17	148.76	155.71	12.90
						155.91	12.96
						156.71	13.85
III-5	155.52	121.22	136.26	124.15	148.76	155.68	12.89
						155.73	12.95
						155.93	13.84
						156.70	

[a] Chemical shifts are referenced to TMS. The resonance peaks are assigned to the italicized carbon atom.

To test if hydrogen bonding is responsible for the multiple conformations found in **II-*n***, the infrared spectra were measured in chloroform solution. The solubility of these materials is quite low so only a limited concentration dependence was possible. (Concentrations ranging between saturated and 20% of saturated gave measurable spectra.) In the N−H stretching region, two narrow peaks were found at 3422 ± 2 and 3323 ± 2 cm^{-1}, invariant with compound. Neither the peak position nor the relative peak intensities changed with dilution. Thus, it appears that intermolecular hydrogen bonding plays, at best, a minor role in influencing the structure in solution. However, intramolecular hydrogen bonding is possible. 2,3-Butandione dihydrazone, which has no azine linkage so exists as a single conformation, has N−H stretches in the IR spectrum at 3325 and 3190 cm^{-1} in both solution and the solid state.[4b] This is quite different from the values found in **II-*n***, making it possible that intramolecular hydrogen bonding is providing a driving force for some of the conformational flexibility found in these compounds.

Some of the differences between **I-*n***, **II-*n***, and **III-*n*** can be explained by looking at the different resonance structures that can contribute to the electronic system in these materials, shown in Scheme 1. The carbonyl bonds in the ketone end groups in **I-*n*** are strongly polarized so that a positive charge can be distributed over the molecule. The lower two resonance structures for **I-*n*** are probably not significant contributors since

Scheme 1

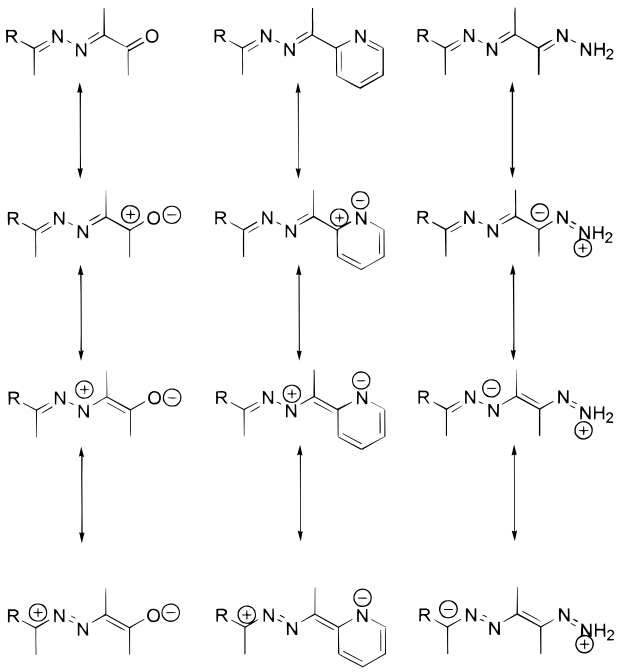

this spreads the charge out over large distances, places a positive charge on nitrogen, and is inconsistent with the observed chemical shifts. Further, since **I-1** is known to have a solid state[2c] structure that is twisted at the

azine N−N bond, accommodation of the resonance structure with the azo-like, −N=N− linkage would be of high energy. The other examples of **I-*n*** also are likely twisted so should follow the same reasoning. In principle, **III-*n*** can also contain charge-separated resonance structures, as shown in Scheme 1, but these resonance structures require breaking the ring aromaticity, and thus should not contribute substantially to the electronic structure of **III-*n***. Finally, in **II-*n*** the hydrazone end groups can only act as electron donors in charge-separated resonance structures. This puts a negative charge on the end group imine carbon, in contrast to **I-*n***.

The experimental data support the resonance structure contributions as discussed in the preceding paragraph. In **I-*n***, the positive charge on the carbonyl carbon atom of the end group causes the adjacent methyl carbon to be deshielded by 10 ppm (compared to the imine methyl groups) in the ^{13}C NMR spectrum. This is further corroborated by the IR spectra of **I-*n*** in chloroform where the carbonyl peaks are found at 1694 ± 2 cm^{-1} (compared to1715 cm^{-1} for the carbonyl peak in 2,3-butanedione[7]). In contrast, the end-group carbons in **III-*n*** have the most shielded resonances, both for the end-group hydrazone carbon (147 ppm) and the attached methyl group (8.6 ppm), consistent with a slight negative charge on the hydrazone carbon atom. The effect of the end-group charges is also detectable in the terminal azine group. The carbon atoms nearest the end group are slightly shielded in **I-*n*** (11.4−11.5 ppm for methyl carbon atoms, 152.4−154.0 for the imine carbon atoms) presumably because the positive charge on the end group attracts electron density from the interior azine groups. The carbon atoms of the azine group nearest the end group in **II-*n*** and **III-*n*** are more deshielded (methyl carbon atoms, 12.4−12.8 ppm in **II-*n***, 13.9 ppm in **III-*n***; imine carbon atoms, 156.6−157.6 ppm, both **II-*n*** and **III-*n***). This is consistent with a small negative charge on the end-group hydrazone carbon in **II-*n*** where the adjacent imine carbon atom becomes polarized slightly positive, leading to the small deshielding. The deshielding of the terminal azine carbon atoms in **III-*n*** is more puzzling. The resonance structures shown in Scheme 1 predict that **III-*n*** should behave more like **I-*n*** but the experimental observations are more like **II-*n***. The most likely explanation for this is that the electron deficient pyridine ring is simply acting as an electronegative group bonded to the terminal azine group.

To test some of these conclusions, semiempirical AM1 calculations were performed for several of the compounds. Results of these calculations are given in Table 3. In all cases, the lowest energy structure found was significantly twisted at both the azine and the diimine linkages, having dihedral angles typically from 95 to 110°. Essentially, the chains are attempting to become helical. However, the C=N and N−N bond lengths are indicative of conjugation, although our experience is that these calculations overestimate the C=N bond lengths by ∼0.04 Å and underestimate the N−N bond lengths by ∼0.06 Å.[2c] The calculations suggest that the preferred structure has the azine N−N bond twisted in such a fashion that the lone pair on one azine nitrogen can conjugate into the neighboring imine bond. This interpretation can account for the large dihedral angles, the short N−N bond, and suggests that electronic information can be communicated along the molecular backbone using both π bonds and N lone pairs. The twisting about the diimine linkage appears to be a result of a combination of steric repulsion between adjacent methyl groups and electrostatic repulsion between nitrogen lone pairs on nearest neighbor azine units. The AM1 calculations give no reasons why the chains with hydrazone end groups have so many more low-energy conformations available.

Table 3. Results of AM1 Calculations for R−[C(CH$_3$)=N−N=C(CH$_3$)]$_n$−R

	ΔH_f^o (kJ/mol)	C=N−N=C[b] (deg)	N=C−C=N[c] (deg)	*r*(C=N) (Å)	*r*(N−N) (Å)
		I-*n* (R = −C(CH$_3$)=O)			
I-1	−127.3	94.5		1.3033	1.3196
I-2	74.8	95.4	100.8	1.3045	1.3194
		95.4		1.3023	1.3193
I-3	257.1	96.5	92.2	1.3034	1.3256
		97.4	95.0	1.3015	1.3225
		106.2		1.3018	
		II-*n* (R = −C(CH$_3$)=N−NH$_2$)			
II-1	428.4	79.2		1.3102	1.3191
				1.3048	
II-2	613.3	110.4	84.8	1.3087	1.3274
		110.5		1.3035	
				1.3023	
II-3	803.5	77.0	116.1	1.3119	1.3228
		81.2	116.3	1.3076	1.3188
		98.8		1.3066	
				1.3045	
		III-*n* (R = 2-pyridine)			
III-1	490.6	115.2		1.3068	1.3176
III-2	696.5	100.4	118.0	1.3065	1.3181
		101.0		1.3046	
III-3	880.8	106.0	94.2	1.3168	1.3408
		106.4	94.6	1.3157	1.3414
		107.0		1.3122	
III-4	1074.6	105.7	93.8	1.3169	1.3414
		106.7	94.2	1.3156	1.3410
		106.9	95.2	1.3152	
		107.0		1.3125	
III-5	1268.3	106.3	94.3	1.3049	1.3263
		106.3	94.3	1.3019	1.3261
		107.0	94.7	1.3019	1.3249
		107.3	94.7	1.3019	
		107.3		1.3018	

[a] Frequency calculations on all structures showed that the reported structures are minima. [b] Azine dihedral angle. [c] Diimine dihedral angle.

The UV spectra demonstrate the strong effect the end groups have on the electronic properties of the oligoazines. Figure 1 displays the UV spectra for **I-3**, **II-3**, and **III-3** as an example (UV spectra for all of the compounds are available in the Supporting Information). Isolated imine bonds typically have a weak n−π* absorption around 230−240 nm (41 700−43 500 cm^{-1}) and an intense π−π* absorption below 220 nm (45 500 cm^{-1}).[8] In contrast, in the solid state the oligoazines normally have two intense π−π* peaks between 250 and 330 nm (40 000 and 30 300 cm^{-1}), depending upon the

(7) Pouchert, C. J. *The Aldrich Library of FT-IR Spectra*; Aldrich Chemical Co.: Milwaukee, WI, 1985; Vol. 1, p 423.

(8) (a) Blout, E. R.; Fields, M. *J. Am. Chem. Soc.* **1948**, *70*, 189−193. (b) Barany, H. C.; Braude, E. A.; Pianka, M. *J. Chem. Soc.* **1949**, 1898−1902. (c) Bonnett, R. *J. Chem. Soc.* **1965**, 2313−2318. (d) Nelson, D. A.; Worman, J. J. *Tetrahedron Lett.* **1966**, 507−509. (e) Sandorfy, C. *J. Photochem.* **1981**, *77*, 297−302.

Table 4. UV−Vis Spectra (CH_3OH) for R−[C(CH_3)=N−N=C(CH_3)]$_n$−R

	azine $\pi-\pi^*$			azine $\pi-\pi^*$			azine $\pi-\pi^*$			azine $\pi-\pi^*$		
	ω_1 (cm^{-1})	$\Delta\omega_1$ (cm^{-1})	ϵ_{max1} ($M^{-1}\,cm^{-1}$)	ω_2 (cm^{-1})	$\Delta\omega_2$ (cm^{-1})	ϵ_{max2} ($M^{-1}\,cm^{-1}$)	ω_3 (cm^{-1})	$\Delta\omega_3$ (cm^{-1})	ϵ_{max3} ($M^{-1}\,cm^{-1}$)	ω_4 (cm^{-1})	$\Delta\omega_4$ (cm^{-1})	ϵ_{max4} ($M^{-1}\,cm^{-1}$)
						I-*n* (R = −C(CH_3)=O)						
I-1[b]							40 680	1 300	9 500	43 500	3 650	10 900
I-2	35 010	2 150	8 630	38 390	894	9 510	39 420	1 620	18 640	42 330	5 895	11 390
I-3	34 110	2 340	19 860	37 720	935	10 450	38 520	1 810	22 270	41 460	5 660	14 030
I-4	33 000	2 210	27 440	37 530	1 130	13 440	37 560	2 580	27 380	43 850	7 040	15 990
						II-*n* (R = −C(CH_3)=N−NH_2)						
II-1				31 730	1 725	6 780	35 730	3 080	14 250	41 460	3 950	7 310
II-2				31 580	2 250	15 380	36 710	2 680	16 250	40 920	5 890	9 930
II-3				31 570	2 310	27 670	36 810	2 480	23 560	40 640	5 950	13 010
						III-*n* (R = 2-pyridine)						
III-1	32 510	1 590	9 770	34 960	1 310	15 190	38 720	2 570	14 890			
III-2	32 650	1 930	21 470	34 820	1 190	9 485	37 780	2 550	21 330			
III-3	31 920	1 840	22 540	34 310	1 025	4 290	36 250	3 290	35 220			
III-4	31 670	1 950	22 310				35 950	3 550	40 120			
III-5	31 620	1 900	36 350				35 760	3 310	53 580			

[a] Parameters for the fitting to Gaussian peaks: ω is the peak maximum, $\Delta\omega$ is the half-width at half-maximum, and ϵ_{max} is the absorptivity at ω. [b] Two additional peaks associated with the carbonyl end group were found: ω = 30 400 cm^{-1}, $\Delta\omega$ = 1 750 cm^{-1}, ϵ_{max} = 180 $M^{-1}\,cm^{-1}$; and ω = 36 000 cm^{-1}, $\Delta\omega$ = 750 cm^{-1}, ϵ_{max} = 500 $M^{-1}\,cm^{-1}$

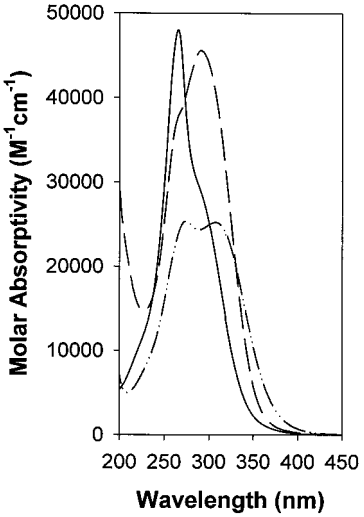

Figure 1. UV spectra (methanol) for **I-3** (solid line), **II-3** (dot−dashed line), and **III-3** (dashed line).

chain length.[1e,2b,3a] The oligoazines reported here follow that pattern but the end groups have a remarkable effect on the relative intensity of the two absorption peaks. Compounds **I-*n***, with the ketone end groups, have the higher energy absorption with large intensity and the lower energy peak as a shoulder. Compounds **III-*n***, with the 2-pyridine end groups, display just the reverse pattern. Finally, **II-*n***, with hydrazone end groups, have two peaks of roughly comparable intensity. These patterns are followed even for the longest chain lengths where, presumably, the end groups should have the least effect.

To better understand these observations, the spectra were deconvoluted into Gaussian line shapes and the results of these fits are given in Table 4. The assignments given in Table 4 were based on the behavior of the peak maximum, line width, and intensity as a function of chain length. **I-1** has two low-energy, low-intensity features that are certainly associated with n−π^* transitions on the carbonyl, similar to 2,3-butanedione. The other features found in all the compounds are assigned to azine $\pi-\pi^*$ transitions because of the large intensities and these lines generally have increasing line width as the chain length increases, as would be expected as a delocalized band is being formed. **III-*n*** does have a pronounced tail into the vacuum UV, which does not provide enough information content to reliably fit, but the maxima associated with these tails must be well above 55 000 cm^{-1} and would seem to be unrelated to the absorptions found in **I-*n*** and **II-*n*** between 30 000 and 44 000 cm^{-1}.

Previously reported calculations on planar, unsubstituted oligo- and polyazines at several levels of theory (Huckel, PPP, Hartree−Fock, and Hartree−Fock crystal orbital)[9] suggest that in the valence orbital energy region there are two filled π levels close in energy (along with at least one nonbonded orbital) and two unfilled π^* levels. For a planar oligoazine with inversion symmetry, only two (of the possible four) $\pi-\pi^*$ transitions are allowed, the HOMO to LUMO and the second highest occupied molecular orbital (HOMO−1) to the second lowest unoccupied molecular orbital (LUMO+1). This means that the two lowest observed bands in a planar (or nearly planar) azine correspond to transitions between the HOMO and LUMO and the HOMO−1 and the LUMO+1. The observation of three or four low energy $\pi-\pi^*$ peaks is consistent with the markedly nonplanar structures found by the AM1 calculations and implied by the NMR results.

Even allowing for significant deviations from planarity, it is puzzling that four peaks were found for **I-*n*** and only three peaks for **II-*n*** and **III-*n***. To explore this further, Hartree−Fock (6-31G(*)) calculations were run on the model compound acetoneazine ($(CH_3)_2$−C=N−N=C$(CH_3)_2$) as a function of the C=N−N=C dihedral angle. For this relatively unhindered model compound, the minimum energy was found for the planar, *s-trans* conformation, although even a dihedral angle of 120° was less than 10 kJ/mol above the minimum. More

(9) (a) Euler, W. B.; Hauer, C. R. *Solid State Commun.* **1984**, *51*, 473−476. (b) Bakhshi, A. K.; Ladik, J. *Solid State Commun.* **1986**, *60*, 361−364. (c) Euler, W. B. *J. Phys. Chem.* **1987**, *91*, 5795−5800. (d) Albert, I. D. L.; Ramasesha, S.; Das, P. K. *Phys. Rev. B* **1991**, *43*, 7013−7019. (e) Nalwa, H. S.; Hamada, T.; Kakuta, A.; Mukoh, A. *Nonlinear Opt.***1993**, *6*, 155−167. (f) Dudis, D. S.; Yeates, A. T.; Kost, D.; Smith, D. A.; Medrano, J. *J. Am. Chem. Soc.* **1993**, *115*, 8770−8774. (g) Schmitz, B. K.; Euler, W. B. *J. Comput. Chem.* **1994**, *15*, 1163−1175.

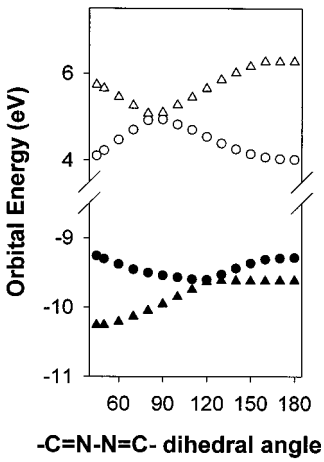

Figure 2. Energies for the HOMO (filled circles), HOMO-1 (filled triangles), LUMO, (open circles), and LUMO+1 (open triangles) for acetoneazine, $(CH_3)_2$—C═N—N═C—$(CH_3)_2$, as a function of the C═N—N═C dihedral angle. The calculations were run at the Hartree−Fock 6-31G(*) level.

importantly, for understanding the electronic spectra, was the effect of the orbital energies as a function of dihedral angle, as shown in Figure 2. Two avoided crossings were found: between the highest two filled levels at about 120° and between the two lowest unoccupied levels at about 90°. In terms of the UV spectra, this means that only two resonances would be found for conformers with dihedral angles near 90°, 120° (because of overlapping but allowed transitions), or 180° (because of symmetry restrictions). The observation of four transitions in the UV spectra for **I-*n*** is consistent with the 102.6° C═N—N═C torsion angle found in **I-1** in the solid-state structure.[2c] Since only three transitions can be identified for **II-*n*** and **III-*n***, it suggests that the C═N—N═C dihedral angle in these compounds is close to 90°, 120°, or 180°, but there is no compelling evidence to point to one angle over another.

Band gaps in conjugated polymers are often estimated by measuring the spectral band edge for a series of oligomers and extrapolating to infinite length.[1e,10] The usual method is to plot the measured band edge against $1/n$ where n is either the number of repeat units or the number of double bonds. The band edge is measured by extrapolating the slope of the low-energy absorption peak to zero absorbance. This gives a fair amount of error, depending upon how the slope is chosen and the influence of the end groups on the spectra. With the deconvoluted spectra, some of this error can be reduced. The lowest energy $\pi-\pi^*$ peak is chosen, removing the effects of any absorption associated with the end groups. The band edge is measured by extending the tangent line at half-maximum to zero absorbance. This gives the band edge as $\omega - 2.027\Delta\omega$, where ω is the peak maximum and $\Delta\omega$ is the half-width at half-maximum, which gives a reproducible method of determining the gap energy. By using the values given in Table 4, the extrapolated band gaps (plotted against $1/n$) for an infinite polyazine with all methyl substituents are 26 480 cm^{-1} for **I**, 26 090 cm^{-1} for **II**, and 27 450 cm^{-1} for **III**, in reasonably good agreement with each other, with an average value of 26 670 ± 1400 cm^{-1} (3.31 ± 0.17 eV, errors are 2σ). This compares to a value of 3.0 eV found previously for poly(methylpropylazine).[3a] The lower value found by using the raw spectra occurs because some of the absorption in the low-energy region of the spectrum arises from the wider, but higher energy transition, thereby artificially broadening the observed line shape.

Conclusion

The nature of the end group has a profound effect on the spectroscopic properties of oligoazines in solution. Ketone and 2-pyridine end groups give simple ^1H and ^{13}C NMR spectra that require that the azines maintain 2-fold symmetry along the chain. In contrast, hydrazone end groups give complicated ^1H NMR spectra but simple ^{13}C NMR spectra, consistent with many conformations present in solution interconverting at room temperature. Semiempirical AM1 calculations suggest that all of these materials are twisted but give no indication why the hydrazone end groups give such different behavior.

The influences of the end groups are also notable in the UV spectra. All three types of end groups give spectra with qualitatively different appearances. However, by deconvolution of the experimental spectra into the line shapes associated with each transition, it is possible to make consistent assignments of the spectra. Further, the parameters derived from the fitting process lead to an estimate of the band gap in polyazine of 3.3 eV, about 10% higher than previous estimates.

Acknowledgment is made to the Chemistry Division of the National Science Foundation, grant CHE-9729819, for support of this work.

Supporting Information Available: UV spectra of all compounds with the Gaussian fits. This material is available free of charge via the Internet at http://pubs.acs.org.

CM9905702

(10) (a) Knoll, K.; Schrock, R. R. *J. Am. Chem. Soc.* **1989**, *111*, 7989−8004. (b) Khanna, R. K.; Jiang, Y. M.; Creed, D. *J. Am. Chem. Soc.* **1991**, *113*, 5451−5453. (c) Khanna, R. K.; Jiang, Y. M.; Srivanas, B.; Smithhart, C. B.; Wertz, D. L. *Chem. Mater.* **1993**, *5*, 1792−1798.